European Journal of Pharmaceutics and Biopharmaceutics 199 (2024) 114300

Contents lists available at ScienceDirect

European Journal of Pharmaceutics and Biopharmaceutics

journal homepage: www.elsevier.com/locate/ejpb

Priming with oncolytic adenovirus followed by anti-PD-1 and paclitaxel treatment leads to improved anti-cancer efficacy in the 3D TNBC model

Lukasz Kuryk [a,*,1], Sara Mathlouthi [b,1], Magdalena Wieczorek [a], Beata Gad [a], Beate Rinner [c], Alessio Malfanti [b], Francesca Mastrotto [b], Stefano Salmaso [b], Paolo Caliceti [b], Mariangela Garofalo [b,*]

[a] Department of Virology, National Institute of Public Health NIH - National Research Institute, Chocimska 24, 00-791 Warsaw, Poland
[b] Department of Pharmaceutical and Pharmacological Sciences, University of Padua, Via F. Marzolo 5, 35131 Padua, Italy
[c] Division of Biomedical Research, Medical University of Graz, Roseggerweg 48, 8036 Graz, Austria

ARTICLE INFO

Keywords:
anti-PD-1
Immunotherapy
Oncolytic adenovirus
TNBC
Paclitaxel
3D-culture
Spheroids
Drug delivery
Nanomedicine

ABSTRACT

Triple-negative breast cancer (TNBC) is considered one of the most incurable malignancies due to its clinical characteristics, including high invasiveness, high metastatic potential, proneness to relapse, and poor prognosis. Therefore, it remains a critical unmet medical need. On the other hand, poor delivery efficiency continues to reduce the efficacy of anti-cancer therapeutics developed against solid tumours using various strategies, such as genetically engineered oncolytic vectors used as nanocarriers. The study was designed to evaluate the anti-tumour efficacy of a novel combinatorial therapy based on oncolytic adenovirus AdV5/3-D24-ICOSL-CD40L with an anti-PD-1 (pembrolizumab) and paclitaxel (PTX). Here, we first tested the antineoplastic effect in two-dimensional (2D) and three-dimensional (3D) breast cancer models in MDA-MB-231, MDA-MB-468 and MCF-7 cells. Then, to further evaluate the efficacy of combinatorial therapy, including immunological aspects, we established a three-dimensional (3D) co-culture model based on MDA-MB-231 cells with peripheral blood mononuclear cells (PBMCs) to create an integrated system that more closely mimics the complexity of the tumour microenvironment and interacts with the immune system. Treatment with OV as a priming agent, followed by pembrolizumab and then paclitaxel, was the most effective in reducing the tumour volume in TNBC co-cultured spheroids. Further, T-cell phenotyping analyses revealed significantly increased infiltration of CD8+, CD4+ T and Tregs cells. Moreover, the observed anti-tumour effects positively correlated with the level of CD4+ T cell infiltrates, suggesting the development of anti-cancer immunity. Our study demonstrated that combining different immunotherapeutic agents (virus, pembrolizumab) with PTX reduced the tumour volume of the TNBC co-cultured spheroids compared to relevant controls. Importantly, sequential administration of the investigational agents (priming with the vector) further enhanced the anti-cancer efficacy in 3D culture over other groups tested. Taken together, these results support further evaluation of the virus in combination with anti-PD-1 and PTX for the treatment of triple-negative breast cancer patients. Importantly, further studies with *in vivo* models should be conducted to better understand the translational aspects of tested therapy.

1. Introduction

Breast cancer remains one of the primary causes of cancer-related deaths among women globally [1]. It is estimated that the number of new cases will increase by over 40% by 2040, resulting in approximately 3 million cases annually [2]. As the most commonly diagnosed cancer in women, it accounts for nearly 12% of all new cancer cases diagnosed in 7.8 million women worldwide [3]. Furthermore, this type of cancer has been categorized into three main subtypes based on the presence of hormonal receptors: estrogen receptor (ER), progesterone receptor (PR), and human epidermal growth factor 2 (HER2) [4].

Triple-negative breast cancer (TNBC) is a subtype of breast cancer that is characterized by the absence of expression of ER and PR receptors as well as the absence of amplification of the HER2 gene. TNBC is

* Corresponding authors.
E-mail addresses: lkuryk@pzh.gov.pl (L. Kuryk), mariangela.garofalo@unipd.it (M. Garofalo).
[1] These authors contributed equally to this work.

https://doi.org/10.1016/j.ejpb.2024.114300
Received 30 January 2024; Received in revised form 5 April 2024; Accepted 18 April 2024
Available online 30 April 2024

considered to be one of the most aggressive types of cancer since it presents more aggressive clinical course, greater tendency to metastasize to other organs, high recurrence risk, and poor survival prognosis [5]. Conventional cancer treatments, such as surgery, radiotherapy, and chemotherapy, have not yielded satisfactory outcomes for this subtype of cancer [6]. However, despite the potential for a better pathologic complete response rate with neoadjuvant chemotherapy, the overall prognosis remains poor [6]. Therefore chemotherapy, primarily consisting of anthracyclines, taxanes, platinum salts, and antimetabolites, is the primary systemic treatment engaged, particularly when surgical resection is not possible or when cancer metastasized throughout the body [7].

Therefore, there is an unmet clinical need to develop more effective treatment strategies for patients with TNBC [8]. In this scenario, oncolytic virotherapy may represent a suitable approach by using genetically modified oncolytic viruses (OVs) that specifically replicate in cancer cells while leaving the healthy ones unharmed [9–15]. Clinical trials testing OVs have shown promising results [16] in terms of safety, however their efficacy as a monotherapy has been modest [16]. In fact, single-agent therapy is rarely successful in treating cancer, especially in metastatic or advanced stages [17–19]. Therefore, combining multiple therapies, both conventional and novel, could enhance anti-cancer performance and represent a promising future for cancer treatment [11,20].

The field of oncology has been revolutionized by the development of immunotherapy agents, such as immune checkpoint inhibitors (ICIs), which have led to durable responses and improvements in overall survival (OS) [21]. Pembrolizumab, an anti-PD-1 antibody, for use in combination with chemotherapy to treat patients with metastatic TNBC whose tumours express PD-L1 [22]. It is also approved as a neoadjuvant treatment for high-risk, early-stage TNBC patients, showing substantial benefit in terms of event-free survival and distant recurrence-free survival, regardless of PD-L1 status [23]. Despite the recent FDA approval of the immune checkpoint inhibitor Atezolizumab, the overall survival benefit of these therapies remains modest [24]. Therefore, multiple association strategies are being evaluated for the treatment of advanced and metastatic stages of TNBC. Unfortunately, the current clinical studies do not compare various treatment approaches, such as sequential or simultaneous administration of oncolytic adenovirus, chemotherapy and pembrolizumab. Clinical studies in TNBC focuses mainly on the combination of two therapeutic agents, including OVs, chemotherapy, tyrosine kinase inhibitors, ICIs [25]. Interestingly it has been shown that a B7-H4 checkpoint-based photodynamic nanodrug combined with neutrophil extracellular traps (NETs) results in a potent therapeutic outcome of TNBC. This combination therapy demonstrates a potent ability in suppressing TNBC growth [26]. Furthermore, recent evidence suggests that OVs may have potential applications against TNBC, particularly when used in combination with ICIs and chemotherapy, to overcome the limitations of single-agent monotherapies [27]. The aim of this study was to assess the anti-tumor effect of a tailored therapy against TNBC, consisting of the oncolytic adenoviral vector AdV5/3-D24-ICOSL-CD40L, the anti-PD-1 monoclonal antibody pembrolizumab (Keytruda) and paclitaxel (PTX), one of the most commonly used chemotherapeutic agents in breast cancer therapies [28]. Therefore, there is a high demand for a proper model that allows for the assessment of diverse interactions between tested agents and the immune and vascular systems [29]. It is important to note that biological barriers to drug transport prevent optimal accumulation of therapeutics specifically at the diseased tumour site, reducing their efficacy. Various limitations, such as off-target distribution, low accumulation, drug instability, and availability still remain unsolved challenges to drug developers [30]. Here, we decided to build a three-dimensional (3D) co-culture model based on MDA-MB-231 cells and peripheral blood mononuclear cells (PBMCs), to create an integrated system, where investigated agents can interact with the immune components. Furthermore, we considered clinically relevant biomarkers that predict response to immunotherapy in TNBC patients [31], such as: PD-L1 expression, tumour-infiltrating lymphocytes (TILs) and tumour mutational burden (TMB). We determined the density of TILs, which presence is considered critical in anti-tumour immunity [32], and sought a potential correlation with the anti-cancer efficacy.

2. Materials and methods

2.1. Cell lines, viruses, anti-PD1 antibody

The study was conducted on several human breast cancer cells provided by Prof. Rinner from the Medical University of Graz (Austria). Luminal A MCF-7 cells and human triple-negative MDA-MB-231 cells were cultured in Dulbecco's Modified Eagle Medium/Nutrient Mixture F-12 (DMEM-F12, Gibco Laboratories, USA) supplemented with 10% fetal bovine serum (FBS, Gibco Laboratories, USA), 1% penicillin/streptomycin (Gibco Laboratories) and 1% L-glutamine (Gibco Laboratories). Human triple negative MDA-MB-468 cells were cultured in Dulbecco's Modified Eagle Medium (DMEM, Sigma, Germany) supplemented with 10% fetal bovine serum (FBS, Gibco Laboratories), 1% penicillin/streptomycin (Gibco Laboratories, USA) and 1% L-glutamine (Gibco Laboratories, USA). The AdV5/3-D24-ICOSL-CD40L, and AdV5/3-D24-mCherry-ICOSL-CD40L (mCherry) adenovirus vectors tested in this study are chimeric serotype 5/3 adenoviruses that were engineered and amplified using AdenoQuick 2.0 Kit (OD260 Inc, Boise, ID, USA) [11,12]. The anti-mouse CD279 (PD1) antibody was purified and resuspended according to the manufacturer's instructions (BioLegend, California, USA). Anti PD-1 antibodies (pembrolizumab) were purchased from Merck.

2.2. Paclitaxel (PTX)

Paclitaxel (PTX; Selleck Chemicals) stock solutions (in DMSO) were dissolved in cell culture medium supplemented with 10% FBS to reach the desired concentration in each well. The concentrations used for two-dimensional (2D) cell culture studies were 0.003 μM, 0.01 μM, 0.03 μM, 0.1 μM, 0.3 μM, 0.5 μM, 1 μM, 3 μM, 5 μM, 7.5 μM and 10 μM, while for three-dimensional (3D) cell culture studies, PTX-cell culture medium solutions at 5 μM, 7.5 μM and 10 μM were used.

2.3. CAR, DSG2 expression in cancer cell lines

MCF-7, MDA-MB-231, and MDA-MB-468 cells were stained with mouse monoclonal anti-CAR antibody (Santa Cruz Biotech, Dallas, TX, USA) followed by 1:2000 Alexa-Fluor 488 secondary antibody (Abcam, Cambridge, UK) or mouse monoclonal anti-DSG2 antibody (Abcam, Cambridge, UK) and then with 1:2000 Alexa-Fluor 488 secondary antibody (Abcam, Cambridge, UK). Flow cytometry analysis was performed using FlowJo v10 software.

2.4. Screening of PTX

Size measurement was performed through dynamic light scattering (DLS) using ZetaSizer (Malvern, Worcestershire, UK) [33–35]. The formulations made of PTX at the highest chosen concentrations (5 μM, 7.5 μM, and 10 μM) were transferred to a polystyrene disposable cuvette in a final volume of the selected cell culture medium (100 μl). A range of concentrations of PTX (PTX; Selleck Chemicals) was tested on a panel of breast cancer cell lines named MCF-7, MDA-MB-231, and MDA-MB-468, seeded at a density of 1×10^4 cells/well in a 96-well plate and kept under standard growth conditions (DMEM-F12/ DMEM, supplemented with 10% FBS, 1% L-glutamine, and 1% penicillin/ streptomycin). After overnight incubation, cells were treated as outlined: 0.003 μM, 0.01 μM, 0.03 μM, 0.1 μM, 0.3 μM, 0.5 μM, 1 μM, 3 μM, 5 μM, 7.5 μM, and 10 μM. Cell viability was assessed 48 and 72 h after treatment using the CellTiter 96 AQueous One Solution Cell Proliferation Assay (MTS) according

to the manufacturer's instructions (Promega, Madison, WI, USA). Absorbance at 490 nm was detected using a 96-well plate spectrophotometer (Victor NivoTM, PerkinElmer). The experiment was performed in triplicate. PTX solubility was assessed at the highest concentrations selected (5 μM, 7.5 μM, and 10 μM) by centrifugation in cell culture medium at 13000 rpm using Hermle Z216 MK centrifuge (Hermle AG, Gosheim, Germany).

2.5. Cell viability: MTS cytotoxicity assay

The MCF-7, MDA-MB-231, and MDA-MB-468 cell lines were seeded at a density of 1×10^4 cells per well in a 96-well plate and maintained under standard growth conditions (DMEM-F12/ DMEM, supplemented with 10% FBS, 1% L-glutamine, and 1% penicillin/streptomycin). After overnight incubation, cells were treated as follows: (i) culture media, (ii) AdV5/3-D24-ICOSL-CD40L (0.1, 1, 10, 100 VP/cell), (iii) PTX 5 μM, (iv) Humanized anti-PD1 antibody pembrolizumab (100 μg/ml), (v) AdV5/3-D24-ICOSL-CD40L (100 VP/cell) + PTX (5 μM), (vi) priming AdV5/3-D24-ICOSL-CD40L (100 VP/cell) + PTX (5 μM), (vii) AdV5/3-D24-ICOSL-CD40L (100 VP/cell) + pembrolizumab (100 μg/ml), (viii) PTX (5 μM) + pembrolizumab (100 μg/ml), (ix) AdV5/3-D24-ICOSL-CD40L (100 VP/cell) + PTX (5 μM) + pembrolizumab (100 μg/ml), (x) priming AdV5/3-D24-ICOSL-CD40L (100 VP/cell) + PTX (5 μM) + pembrolizumab (100 μg/ml). Table 1 presents the treatment schedule. Cell viability was assessed 96 h after treatment using the CellTiter 96 AQueous One Solution Cell Proliferation Assay (MTS) according to the manufacturer's instructions (Promega, Madison, WI, USA). Absorbance at 490 nm was detected using a 96-well plate spectrophotometer (Victor Nivo™, PerkinElmer). The experiment was performed in triplicate.

2.6. Immunogenic cell death (ICD)

CRT exposure. Cell lines were seeded in duplicate onto 6 well plates at a density of 5×10^5 cells/well. The cells were treated according to the groups listed in Table 1. After 60 h, cells were collected and stained with a 1:1000 dilution of rabbit polyclonal anti-Calreticulin antibody (Abcam, Cambridge, UK) for 40 min at 4 °C, followed by flow cytometry analysis (Franklin Lakes, NJ, USA) [9].

ATP release. Cell lines were seeded in triplicate onto 96 well plates at a density of 1×10^4 cells/well and treated as described in Table 1 above. After 96 h, supernatants were recovered, and luminometric analysis was performed using the ATP Determination Kit (Promega, Madison, WI) according to the manufacturer's procedure (Varioscan Flash, ThermoFisher Scientific, Waltham, MA) [9].

Table 1
Treatment schedule for the assessment of tested anti-cancer agents *in vitro*.

Treatment conditions	Day 1 (24 h after seeding)	Day 2 (48 h after seeding)
Pembrolizumab	100 μg/mL	Treatment removal
AdV5/3-D24-ICOSL-CD40L	100 VP/cell	
Paclitaxel	5 μM	
AdV5/3-D24-ICOSL-CD40L + Pembrolizumab	100 VP/cell + 100 μg/mL (Pembro)	
Co-adm. AdV5/3-D24-ICOSL-CD40L + Paclitaxel	100 VP/cell + 5 μM (PTX)	
Co-adm. AdV5/3-D24-ICOSL-CD40L + Paclitaxel + Pembrolizumab	100 VP/cell + 100 μg/mL (Pembro) + 5 μM (PTX)	
Priming AdV5/3-D24-ICOSL-CD40L + Paclitaxel	100 VP/cell	Treatment removal + 5 μM PTX
Pembrolizumab + Paclitaxel	100 μg/mL (Pembro)	
Priming AdV5/3-D24-ICOSL-CD40L + Pembrolizumab + Paclitaxel	100 VP/cell + 100 μg/mL (Pembro)	

2.7. Confocal microscopy

MCF-7, MDA-MB-231, and MDA-MB-468 cells were seeded on 24-chamber glass slides (Sigma–Aldrich, St. Louis, MO, USA) in a 24 well plate at a concentration of 10^5 cells/well in the appropriated cell culture medium. After 24 h cells were treated as follows: (i) AdV5/3-D24-ICOSL-CD40L mCherry (100 VP/cell), (ii) PTX (5 μM), (iii) AdV5/3-D24-ICOSL-CD40L (100 VP/cell) + PTX (5 μM), priming AdV5/3-D24-ICOSL-CD40L (100 VP/cell) + PTX (5 μM). After 24, 48 and 72 h, cells were washed three times with PBS (Aurogene, Rome, Italy) and then fixed with 4% (w/v) paraformaldehyde in PBS for 15 min. Nuclei were stained with Hoechst (Thermo Scientific, Waltham, Massachusetts, USA) diluted 1:1000 in PBS and incubated for 10 min. Cells were washed three times with PBS between these steps. Cover glasses were removed from plates and mounted in microscope slides (Menzel-Glaser, Thermo Scientific, Waltham, Massachusetts, USA) using Prolong™ Glass Antifade mountant (InVitrogen, Waltham, Massachusetts, USA). A confocal analysis was performed by Zeiss LSM800 (Zeiss, Oberkochen, Germany) equipped with 63x oil objective. Lasers at 385/30 nm and 631/33 nm were used to detect the fluorescence of DAPI and mCherry, respectively. Image analyses were carried out using ImageJ.

2.8. Establishment of 3D-cell culture

For spheroids formation, the MCF-7 breast cancer cell line and the triple-negative breast cancer cell lines MDA-MB-231 and MDA-MB-468 were seeded at varying densities (1000 – 2000 – 3000 – 5000 – 7500 – 10,000 cells/well) in 96-well plates with a flat bottom. The plates were previously coated with 50 μl of 1.5% agarose solution (Thermo Scientific, Waltham, Massachusetts, USA). After seeding, the plates were centrifuged at 1000 rpm for 5 min. Then, spheroid's morphology and growth were monitored using Axiovert 40 CFL microscope (Zeiss, Oberkochen, Germany) for 9 days both for MCF-7 and MDA-MB-468 cell lines while for 12 days for MDA-MB-231 cells. Spheroid areas were registered every three days using imaging software (AxioVision software by Zeiss, Oberkochen, Germany). The volume of the 3D tumour spheroids was calculated based on measurements of their orthogonal diameters using the formula $0.52 \times \text{length} \times (\text{width})^2$.

2.9. 3D-cell culture spheroids: PTX and oncolytic adenovirus screening

MCF-7, MDA-MB-231 and MDA-MB-468 cells were seeded at a density of 2000 cells/well on a 96 well plate, previously coated with 50 μl of 1.5% agarose solution. After 8 days from spheroids formation, treatments were performed as follows: (i) culture media, (ii) PTX 5 μM, (iii) PTX 7.5 μM, (iv) PTX 10 μM, (v) AdV5/3-D24-ICOSL-CD40L 10^8 VP/ml and (vi) AdV5/3-D24-ICOSL-CD40L 10^9 VP/ml. Spheroid areas were registered every three days using imaging software (AxioVision software by Zeiss, Oberkochen, Germany).

2.10. 3D-cell culture spheroids treatment

MCF-7, MDA-MB-231 and MDA-MB-468 cells were seeded onto a 96 well plate, previously coated with 50 μl of 1.5% agarose solution, at a density of 2000 cells/well. After 8 days from spheroids formation, treatments were performed as outlined in Table 2. Spheroid areas were registered every three days using imaging software (AxioVision software by Zeiss, Oberkochen, Germany). The volume of the 3D tumour spheroids was calculated based on measurements of their orthogonal diameters using the formula $0.52 \times \text{length} \times (\text{width})^2$.

2.11. Establishment of 3D co-cultures of MDA-MB-231 cells with peripheral blood mononuclear cells (PBMCs)

PBMCs were purchased from Stemcell Technologies (Vancouver, British Columbia, Canada) prior to the experiment and stored in liquid

Table 2
Treatment schedule for 3D cell culture breast cancer models.

Conditions/Days	Day 0	Day 7	Day 10	Day 13	Day 16	Day 19	Endpoint
CTRL	Cells seeded on a 96 well plate previously coated with 1.5% agarose at a rate of $2x10^3$ cells/well	Medium change					Follow up until day 31 Medium change once a week Size and dimensions registered every 3 days
AdV5/3-D24-ICOSL-CD40L		10^9 VP/ml	10^9 VP/ml	10^9 VP/ml	Medium change	10^9 VP/ml	
Paclitaxel		10 μM	10 μM	10 μM	Medium change	10 μM	
Co-adm. AdV5/3-D24-ICOSL-CD40L + Paclitaxel		10^9 VP/ml + 10 μM	10^9 VP/ml + 10 μM	10^9 VP/ml + 10 μM	Medium change	10^9 VP/ml + 10 μM	
Priming AdV5/3-D24-ICOSL-CD40L + Paclitaxel		10^9 VP/ml	10 μM	10^9 VP/ml	10 μM	10^9 VP/ml	

nitrogen until they were used in co-culture with the cancer cells. The MDA-MB-231 cells were stained, according to the manufacturer's instructions, with carboxyfluorescein succinimidyl ester (CFSE, Sigma-Aldrich, Saint Louis, MO, USA) while the CellTracker Orange CMTMR (C2927, Invitrogen, Waltham, Massachusetts, USA) was used to stain PBMCs, following the manufacturer's instructions. MDA-MB-231 cell lines, previously stained with cell trace CFSE, were seeded at a density of 1000 cells/well in 96-well plates with a flat bottom, previously coated with 50 μl of a 1.5% agarose solution (Thermo Scientific, Waltham, Massachusetts, USA). After seeding, the plates were centrifuged at 1000 rpm for 5 min to allow spheroid formation. On day 6, co-culture was assembled, and PBMCs, already stained with CellTracker Orange, were added to the spheroids in a 1:1 ratio (MDA-MB-231 cancer cells count was equal to PBMCs count). After 24 h, images were acquired using a 10x fluorescence microscope objective (Nikon Ts).

2.12. 3D co-culture combination therapy

MDA-MB-231 cells were seeded at a density of 1000 cells/well on a 96 well plate previously coated with 50 μl of a 1.5% agarose solution. On day 6, after spheroid formation, the PMBCs infiltration inside tumour cell-spheroids was performed as previously described [32] in a 1:1 ratio. On day 7, the cells were treated as outlined in Table 3. Spheroids were treated as follows: (i) culture media, (ii) AdV5/3-D24-ICOSL-CD40L (10^9 VP/ml), (iii) PTX 10 μM, (iv) Humanized anti-PD1 antibody pembrolizumab (150 μg/ml), (v) AdV5/3-D24-ICOSL-CD40L (10^9 VP/ml) + PTX (10 μM), (vi) priming AdV5/3-D24-ICOSL-CD40L (10^9 VP/ml) + PTX (10 μM), (vii) AdV5/3-D24-ICOSL-CD40L (10^9 VP/ml) + pembrolizumab (150 μg/ml), (viii) PTX (10 μM) + pembrolizumab (150 μg/ml), (ix) AdV5/3-D24-ICOSL-CD40L (10^9 VP/ml) + PTX (10 μM) + pembrolizumab (150 μg/ml), (x) priming AdV5/3-D24-ICOSL-CD40L (10^9 VP/ml) + PTX (10 μM) + pembrolizumab (150 μg/ml). The treatments were administered every three days, and the culture medium was changed once a week. The size of the spheroids was measured every three days on two dimensions while the volume was calculated using the formula 0.52 × length × $(width)^2$. The area was measured using AxioVision software by Zeiss.

2.13. Immune cell infiltrates – In vitro analysis

The percentage of human immune cell populations was monitored using flow cytometry, as described earlier [36]: human: CD45+ lymphocytes (BD, cat. number: 564105), T cells hCD3+ (BD, cat. number: 555339), CD4+ T cells (hCD3+ hCD4+, BD, cat. number: 557852), CD8+ T cells (hCD3+ hCD8+, BD, cat. number: 560179), FoxP3 (hCD3+ hCD4+ hFoXP3+, BD, cat. number: 560046). Spheroids were harvested and subsequently dissociated to obtain a suitable number of cells for further T cell phenotyping analyses. After dissociation, cells were washed with BD Perm/Wash™ buffer (cat. no. 554723) and stained with antibodies for 30 min at 4 °C in the dark and then suspended in stain buffer FBS (BD, cat no. 554656). Samples were acquired using BD Lyric FACS Flow. The populations were gated with forward and side scattering (FSC-A/SSC-A dot plot) in leukocytic regions. Flow cytometry analysis was performed using FlowJo v10 software.

2.14. Statistical analysis

GraphPad Prism software (Version 9) was used to analyse *in vitro* and

Table 3
Treatment schedule for the 3D co-culture model aiming at studying anti-cancer potential of investigated agents.

Conditions/Days	Day 0	Day 7	Day 10	Day 13	Day 16	Day 19	Endpoint
CTRL	Cells seeded on a 96 well plate previously coated with 1.5% agarose at a rate of $2x10^3$ cells/well	Medium change					Follow up until day 31 Medium change once a week Size and dimensions registered every 3 days
Paclitaxel		10 μM	10 μM	10 μM	Medium change	10 μM	
Paclitaxel + Pembrolizumab		10 μM + 150 μg/mL	10 μM + 150 μg/mL	10 μM + 150 μg/mL	Medium change	10 μM + 150 μg/mL	
AdV5/3-D24-ICOSL-CD40L		10^9 VP/ml	10^9 VP/ml	10^9 VP/ml	Medium change	10^9 VP/ml	
Pembrolizumab		150 μg/mL	150 μg/mL	150 μg/mL	Medium change	150 μg/mL	
AdV5/3-D24-ICOSL-CD40L + Pembrolizumab		10^9 VP/ml + 150 μg/mL	10^9 VP/ml + 150 μg/mL	10^9 VP/ml + 150 μg/mL	Medium change	10^9 VP/ml + 150 μg/mL	
Co-adm. AdV5/3-D24-ICOSL-CD40L + Paclitaxel		10^9 VP/ml + 10 μM	10^9 VP/ml + 10 μM	10^9 VP/ml + 10 μM	Medium change	10^9 VP/ml + 10 μM	
Co-adm. AdV5/3-D24-ICOSL-CD40L + Paclitaxel + Pembrolizumab		10^9 VP/ml + 150 μg/mL + 10 μM	10^9 VP/ml + 150 μg/mL + 10 μM	10^9 VP/ml + 150 μg/mL + 10 μM	Medium change	10^9 VP/ml + 150 μg/mL + 10 μM	
Priming AdV5/3-D24-ICOSL-CD40L + Paclitaxel		10^9 VP/ml	10 μM	10^9 VP/ml	10 μM	10^9 VP/ml	
Priming AdV5/3-D24-ICOSL-CD40L + Pembrolizumab + Paclitaxel		10^9 VP/ml + 150 μg/mL	10 μM	10^9 VP/ml + 150 μg/mL	10 μM	10^9 VP/ml + 150 μg/mL	

in vivo variables. Statistical analysis employed repeated measures one-way and two-way ANOVA tests. The Pearson correlation coefficient was used to investigate possible correlations between tumour volume and the percentage of CD4+, CD8+, and Tregs cells in tumour-infiltrating lymphocytes (spheroids).

3. Results and discussion

3.1. Expression of Coxsackie-Adenovirus receptor (CAR) and Desmoglein-2 (DSG2) receptors in human breast cancer cells

To assess the possibility of using the oncolytic adenovirus AdV5/3-D24-ICOSL-CD40L to treat TNBC, we first evaluated the expression of adenoviral receptors on a panel of different human breast cancer cells: MCF-7, a luminal A cell line used as control since it is hormone-receptor positive [37], and MDA-MB-231 and MDA-MB-468, which were chosen as metastatic triple-negative cell lines. The expression levels of the Coxsackievirus and Adenovirus (CAR) and Desmoglein-2 (DSG2) receptors were investigated first, since the chimeric nature of the fiber protein of the AdV5/3-D24-ICOSL-CD40L can exploit both CAR and DSG2 receptors to enter cells, thus enhancing the chances of viral uptake. The breast cancer cell lines (MCF-7, MDA-MB-231, and MDA-MB-468) expressed higher levels of DSG2 on their surfaces (99%, 70%, and 95%, respectively) compared to CAR (56%, 9.8%, and 70%, respectively) (see Supplementary Fig. 1). Therefore, since DSG2 is a receptor for adenovirus 3, 7, and 11, we have engineered a chimeric AdV5/3 fiber knob to successfully infect cancer cells, targeting overexpressed membrane proteins DSG [38–40]. The obtained results are in agreement with previous findings reporting that oncolytic adenovirus internalization mainly occurs via interaction with DSG2 receptors [11,40]. The vector did not reduce the viability of PBMCs (data not shown).

3.2. Screening of PTX in two-dimensional (2D) breast cancer models

To assess the feasibility of a combination therapy based on AdV5/3-D24-ICOSL-CD40L combined with pembrolizumab and PTX, for the treatment of TNBC, before assessing the possible anti-cancer efficacy of the combination therapy in two-dimensional (2D) cell culture, we first needed to perform a proper screening of the PTX behavior alone (see Supplementary Fig. 2). Prior to conducting the *in vitro* assays, we made sure that PTX, drug with poor solubility, was solubilized within the wells even at the highest concentrations (5; 7.5; 10 μM) to avoid the formation of aggregates which will then result in a precipitation (Supplementary Fig. 2A). The results indicate that the highest cytotoxic activity for PTX was registered in MCF-7 and MDA-MB-231 cell lines Supplementary Fig. B-C) thus suggesting that the MDA-MB-468 line may be more resistant to PTX treatment (Supplementary Fig. D) [41]. The selection of the proper suboptimal dose of tested agents played a crucial role in our experimental design when evaluating synergism. Therefore, based on dosing studies aimed at seeking a potential synergistic or additive anti-cancer effect for a combinatorial therapy, we have decided to choose a suboptimal dose of PTX (5 μM PTX). After 72 h of treatment with 5 μM of PTX, cell viability was reduced to below 30% (22.92% for MCF-7, 12.24% for MDA-MB-231 and 27.91% for MDA-MB-468) in all the examined cell lines, as a concentration to be tested in combination with the oncolytic vector in upcoming experiments.

3.3. Evaluation of cell cytotoxicity and transduction efficiency in 2D in vitro culture model

The *in vitro* cytotoxicity of AdV5/3-D24-ICOSL-CD40L was tested in breast cancer cells (MCF-7, MDA-MB-231, and MDA-MB-468) (see Supplementary Fig. 3). The results demonstrate the oncolytic potency of tested AdV5/3-D24-ICOSL-CD40L in all tested cancer cell lines (Supplementary Fig. 3).

To evaluate the oncolytic potency of AdV5/3-D24-ICOSL-CD40L in combination with PTX and pembrolizumab, MTS cell viability assays were performed on breast cancer cells (Fig. 1). Since each virus belonging to different species has its own timing of attachment, internalization, infection, and replication inside cells, we firstly needed to figure out whether the oncolytic effect of AdV5/3-D24-ICOSL-CD40L could be affected by the co-administration of an antimitotic agent such as PTX [41]. After determining the proper dose of each anti-tumoral agent (see Supplementary Figs. 2 and 3) we tested two different modalities of co-administration. The first one involved simultaneous administration of both PTX and the oncolytic adenovirus, while the second one considered the viral absorption time, needed for its attachment to the cell surface and consequent internalization. For this reason, the first step was to administer only the virus or the vector plus pembrolizumab (as priming agents) and subsequently adding the PTX 48 h post priming, thus leaving the virus and anti-PD-1 sufficient time to carry out their anti-cancer therapeutic effect. Then, once PTX is added, it acted by inhibiting the depolymerization of the mitotic spindle and consequently the cell division. The treatment scheme for breast cancer cells is presented in Table 1. The results indicate that MDA-MB-231 is the most responsive cell line, with a consistent reduction in cell viability (co-administration AdV5/3-D24-ICOSL-CD40L + PTX + pembrolizumab: 29.21% *vs* priming AdV5/3-D24-ICOSL-CD40L + PTX + pembrolizumab: 14.54%) (Fig. 1C). However, the combination therapy, particularly when using the priming agents combined with PTX, was able to induce higher tumour cell death in all tested cell lines compared to single monotherapies (Fig. 1). As anticipated, the inclusion of pembrolizumab did not enhance the cell viability in this 2D mono-cell system.

Confocal microscopy analysis was performed to assess the effect of AdV5/3-D24-ICOSL-CD40L (expressing mCherry) and its combination with PTX on breast cancer cells, by the assessment of the transfection through fluorescent protein visualization (Fig. 2). The progress of the viral infection could be monitored by detecting the emission signal of the protein fluorophore mCherry (excitation λ: 540–590 nm; emission λ: 550–650) which is expressed by the virus. The more intense the emission of this signal, the greater the concentration of the fluorophore, and consequently the presence of the actively replicating oncolytic virus inside tumour cells. Confocal analysis revealed the morphological changes induced by PTX already after 24 h in all tested cell lines (Fig. 2A-C). In fact, the drug was able to induce polynucleation, resulting in tumour cells with a more rounded shape, typical of prometaphase in which they are frozen [42]. Furthermore, the obtained findings demonstrated a higher effectiveness of PTX as compared to the oncolytic adenovirus alone (Fig. 2A-C). In fact, PTX is a first-line chemotherapeutic agent for treating triple-negative breast cancer. This chemotherapeutic suppresses the polymerization dynamic of microtubules, resulting in the induction of mitotic arrests due to the activation of the mitotic checkpoint [43,44]. Additionally, it is important to note that both agents exhibit different modes of action, where chemotherapy is more rapidly causes cell death, while adenoviruses require more time to replicate and lyse cells. Therefore, it is crucial to consider an optimal therapeutic window. Interestingly, in MDA-MB-231 cells, the number of cells decreases following the combination treatment schedule (Fig. 2E). This result is especially noticeable when priming the virus in combination with PTX (Fig. 2E), which is consistent with the results obtained from cell viability studies (Fig. 1). Taken together, these findings suggest that the sequential administration of priming agents combined with chemotherapy demonstrates an improved anti-cancer effect compared to the concomitant treatment scheme against breast cancer lines with different characteristics.

3.4. Immunogenic cell death assessment

Markers for immunogenic cell death (ICD), such as the exposure of calreticulin (CRT) to the cell surface and the extracellular release of ATP were measured from breast cancer cell cultures after exposure to the

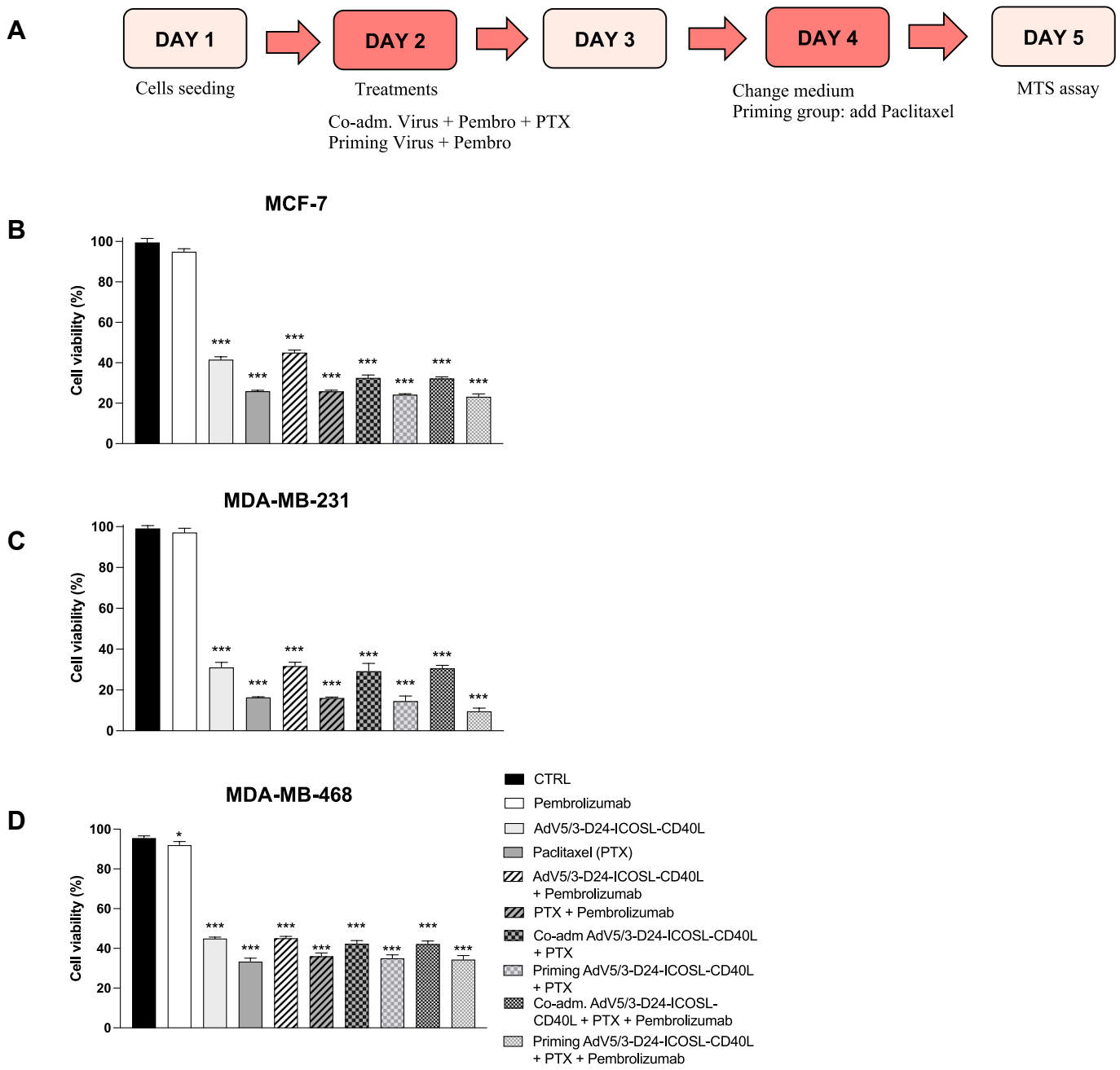

Fig. 1. Evaluation of combination therapy through MTS cytotoxicity assay. Different combinations of AdV5/3-D24-ICOSL-CD40L 100 VP/cell, PTX 5 μM, and pembrolizumab 100 μg/ml were tested on MCF-7, MDA-MB-231, and MDA-MB-468 after 72 h. Data are expressed as the percentage of viable cells, determined using CellTiter 96 Aqueous One Solution Cell Proliferation Assay (MTS) and measuring the absorbance at 490 nm with a 96-well plate spectrophotometer Viktor Nivo™. Statistical analysis was performed with *t*-test (***P ≤ 0.001).

virus, PTX, and pembrolizumab as monotherapies and in combination (Fig. 3). Immunogenic cell death was observed when cells were treated with the virus and combinatory therapy, especially in priming settings with the vector. The study demonstrated the superiority of the priming protocol using AdV5/-D24-ICOSL-CD40L followed by PTX combination over the co-administration treatment regime (whether double or triple combinations) (Fig. 3). Moreover, the release of ATP in PTX monotherapy was also high, particularly in MDA-MB-231 (66.49%) and MCF-7 (69.76%) cell lines (Fig. 3A, 3B). Thus, the results reveal that all tested cell lines were susceptible to induction of ICD when treated with combinatory therapies, OV and PTX alone, but not pembrolizumab. In fact, immunotherapy such as oncolytic viruses constitute of immunogenic anti-cancer therapy that sensitizes to subsequent immune checkpoint blockade. Therefore, combining sequential treatment with checkpoint inhibition of PD-1 can lead to a more potent antineoplastic effect on primary lesions and distant tumours, emphasizing the potency of combining ICD induction with checkpoint blockade [45].

3.5. *Three-dimensional 3D breast cancer models*

In order to validate novel therapies, it is crucial to develop systems that are able to simulate tumour behavior and characteristics, bearing in mind that monolayered cultures poorly reproduce the complexity of TME [46]. Therefore, to further investigate the effectiveness of the proposed anti-cancer therapies for TNBC, human 3D spheroids of breast cancer cells have been formed, aiming to mimic a hypothetical *in vivo*

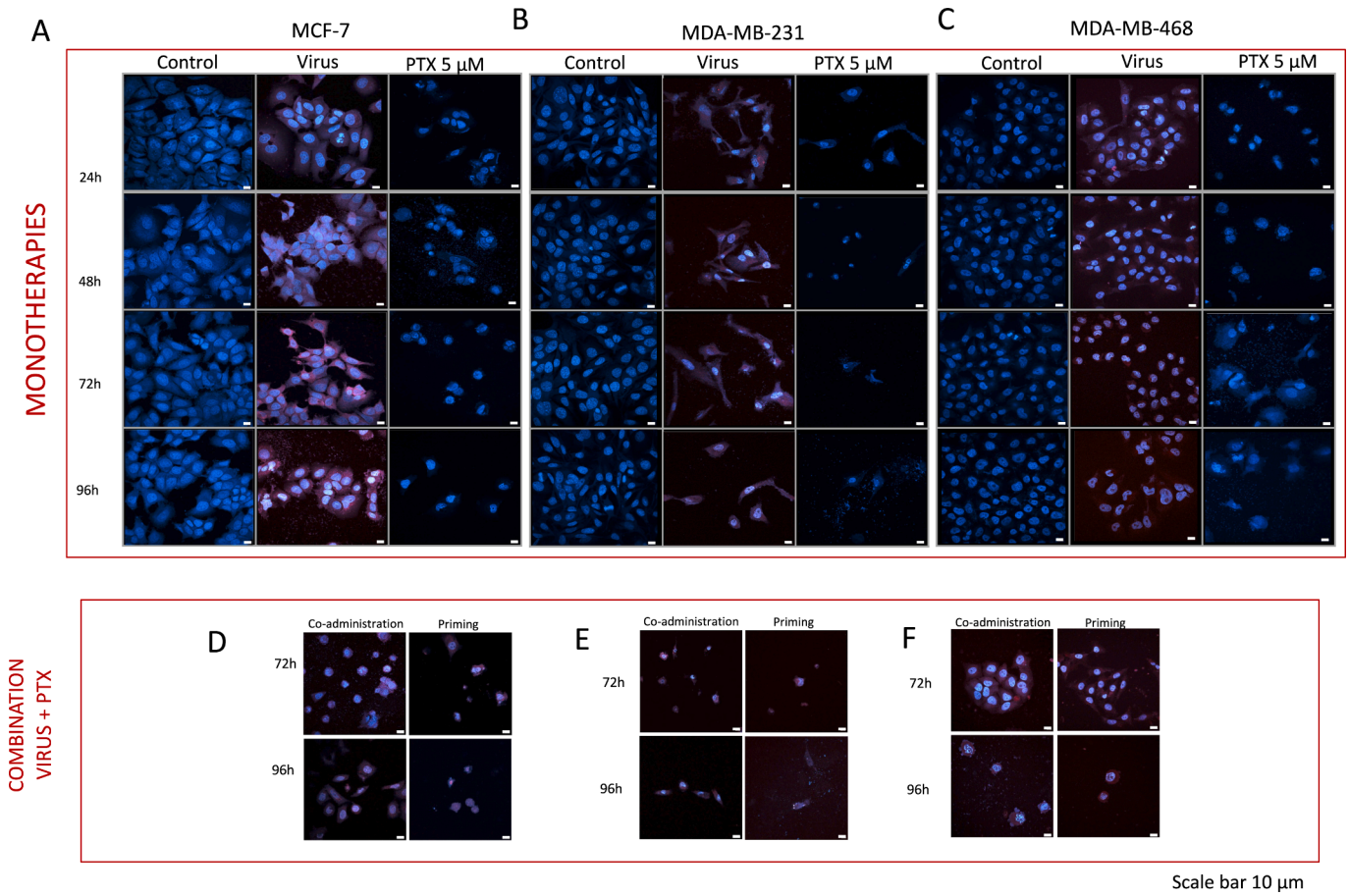

Fig. 2. Transduction efficiency assessed by confocal microscopy. Breast cancer cells MCF-7, MDA-MB-231, and MDA-MB-468 were seeded onto 24-chamber glass slides (Sigma–Aldrich, St. Louis, MO, USA) in a 24 well plate at a concentration of 10^5 cells/well. After incubation for 24, 48, and 72 h respectively, the cells were washed three times with PBS (Aurogene) and fixed with 4% (w/v) paraformaldehyde in PBS for 15 min. The nuclei were stained with Hoechst (Thermo Scientific) diluted 1:1000 in PBS, and incubated for 10 min. Confocal analysis was conducted using a Zeiss LSM800 microscope with 63x oil objective. Fluorescence of Hoechst and mCherry was detected using lasers at 385/30 nm and 631/33 nm, respectively.

treatment, performing multiple administrations of the drug agents and a long-term follow-up, which included the measurements of spheroid integrity and growth kinetics by registering both the areas (μm^2) and the tumour volume (mm^3). Regarding the most appropriate day to start the different treatments, it was hypothesised that all cell lines could be treated around day 7–8 post spheroid formation, since the spheroids are all in the linear growth phase and the initial phenomenon of spheroid area reduction, which is particularly evident in the setting of spheroids composed of MDA-MB-231 cells (Supplementary Fig. 4), cannot be considered as an effect of the administered anti-cancer drug agents.

First, a dose screening for PTX and virus, both as monotherapies, was performed to further understand how the change in cellular structure from two-dimensional culture systems to aggregated 3D systems might affect the diffusion and consequently the efficacy of the anti-cancer drug (Supplementary Fig. 5). Considering that spheroids tend to be a resistant system with lower permeability and diffusion of the drug, they may require higher dosages comparable to those used in *in vivo* treatments [47]. Therefore, breast cancer spheroids were established (Supplementary Fig. 5A) and treated with virus alone and PTX alone. The results showed that the highest concentration of the virus (10^9 VP/ml) and PTX (10 μM) were able to efficiently reduce spheroid areas in all treated cell lines (Supplementary Fig. 5B-C-D). Interestingly, there was a rebound in spheroids size in all PTX treated groups once the treatments were suspended. This behavior seems to resemble what commonly occurs in *in-vivo* experiments [48,49].

In order to better characterize the effect of both single (PTX, pembrolizumab, AdV5/3-D24-ICOSL-CD40L) and combinatorial therapies, 3D culture models were also investigated. Breast cancer spheroids have been treated according to the scheme presented in Table 2. We didn't add pembrolizumab at that stage because the spheroids were still a mono-system, composed of tumour cells, and there was no immune component with which the ICI could interact properly.

The results obtained confirm the improved anti-cancer efficacy of AdV5/3-D24-ICOSL-CD40L, especially in the MDA-MB-231 cell line as compared to the other breast cancer models tested (Fig. 4D). Furthermore, once treatments were completed, the virus was able to further reduce the tumour volume of the spheroid by day 33, thus demonstrating its long-term efficacy (MCF-7: tumour volume: 0.0227 mm^3; MDA-MB-231: tumour volume: 0.0032 mm^3; MDA-MB-468: tumour volume: 0.03576 mm^3) (Fig. 4C-E) compared to untreated control spheroids (MCF-7: tumour volume: 0.104 mm^3, MDA-MB-231: tumour volume: 0.294 mm^3, MDA-MB-468: tumour volume: 0.107 mm^3) and PTX treated spheroids (MCF-7: tumour volume: 0.059 mm^3, MDA-MB-231: tumour volume: 0.052 mm^3, MDA-MB-468: tumour volume: 0.081 mm^3).

In the case of MDA-MB-468, the virus was less effective, but was still able to control tumour volume throughout the entire observation period (Fig. 4E, Supplementary Fig. 6C). Interestingly, the combination therapies showed an enhanced anti-cancer effect compared to the monotherapies, especially when the virus was used as a priming agent followed by the addition of PTX 48 h post-infection, this effect was registered especially in the MDA-MB-231 and MCF-7 cell lines (Fig. 4D-E, Supplementary Fig. 6A-B). We can speculate that the effect of pembrolizumab (prevention of T cell inhibition) has synergized anti-cancer

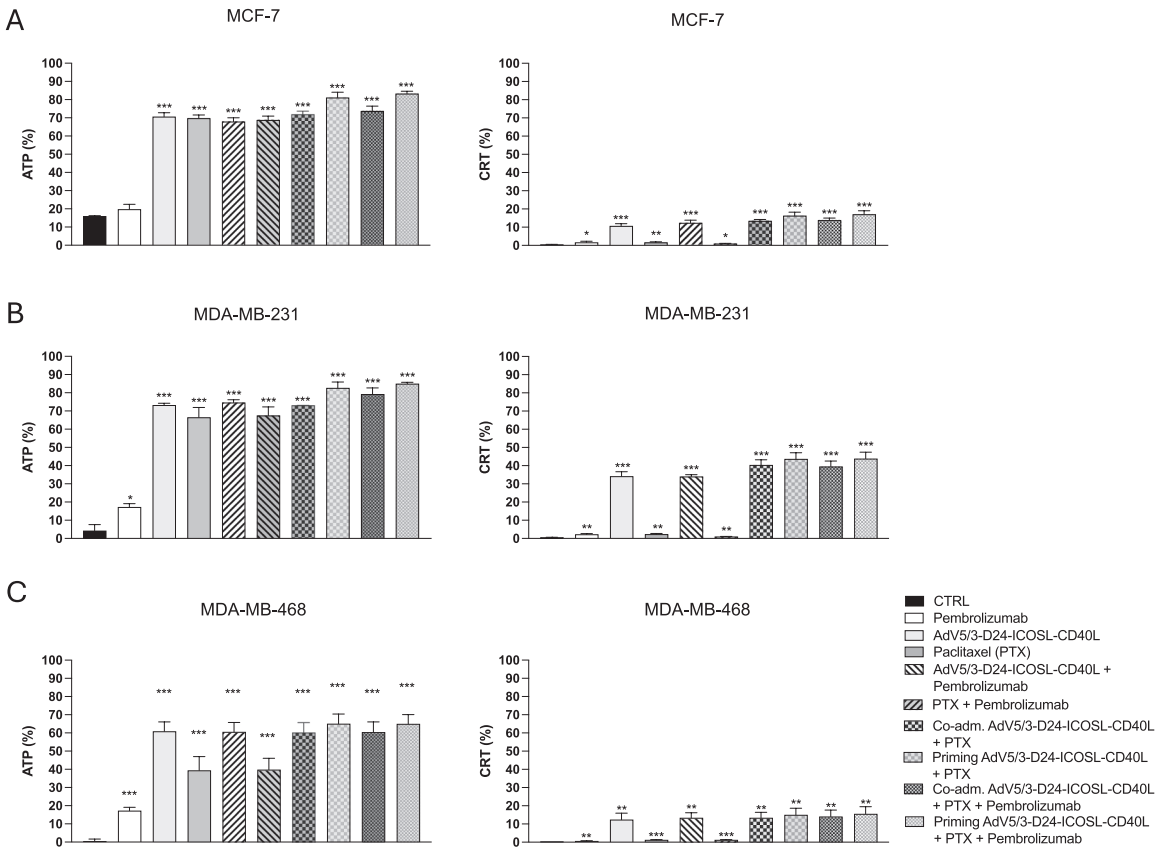

Fig. 3. Immunogenicity of cell death. ATP levels were detected 72 h after infection with AdV5/3-D24-ICOSL-CD40L at the concentration of 100 VP/cell of a) MCF-7, b) MDA-MB-231 and c) MDA-MB-468. Data are expressed as the % of extracellular ATP, assessed with ATP determination kit CellTiter-Glo® Luminescent Cell Viability Assay (Promega), the luminescence was then assessed with Viktor NivoTM. CRT levels were detected 48 h after infection with AdV5/3-D24-ICOSL-CD40L at the concentration 100 VP/cell. Data are expressed as the % of positive cells for CRT, measured by flow cytometry (BD FACSAria III, Becton Dickinson, USA) followed by specific antibody staining. Statistical analysis was performed with *t*-test (*P ≤ 0.05, **P ≤ 0.01, ***P ≤ 0.001).

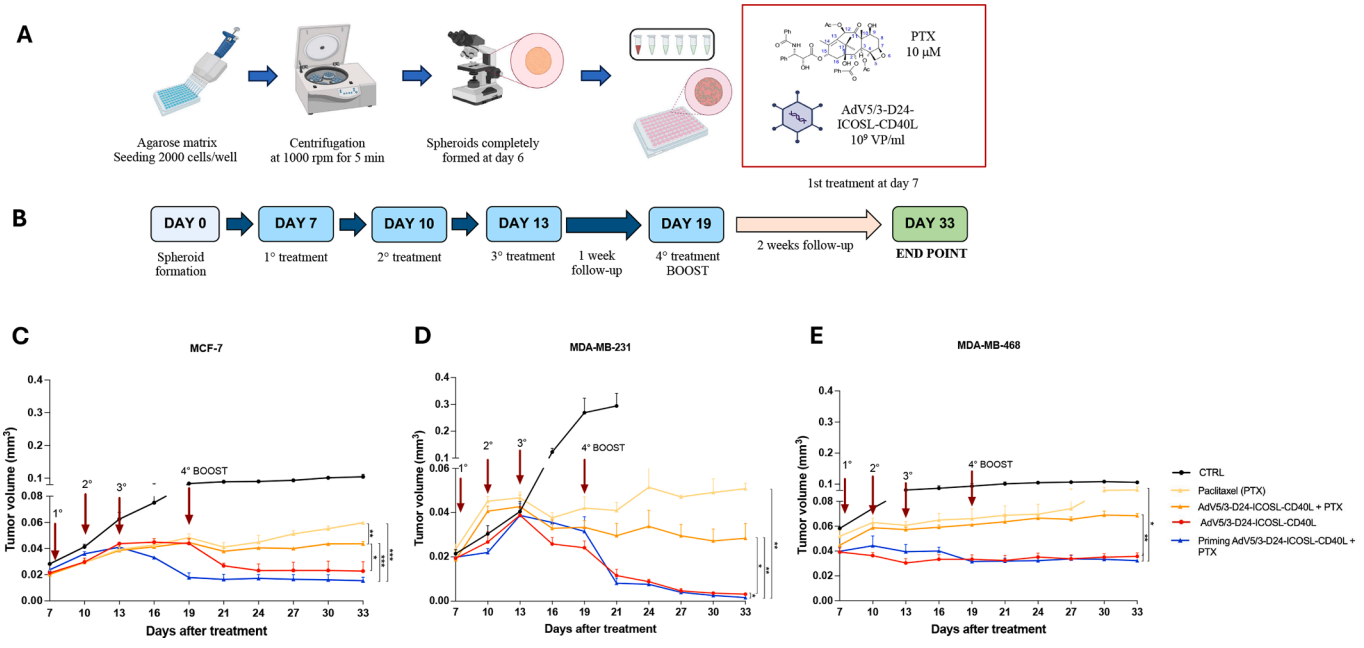

Fig. 4. Efficacy of combination therapy based on AdV5/3-D24-ICOSL-CD40L and PTX in 3D breast cancer spheroids. (A-B) Scheme of the protocol for the establishment and treatment of 3D *in vitro* breast cancer spheroids. (C-D-E) MCF-7, MDA-MB-231, and MDA-MB-468 spheroids were treated with four administration of AdV5/3-D24-ICOSL-CD40L (10^9 VP/cell), PTX (10 μM) and their combination using the priming and co-administration protocol. Tumour volume was obtained by applying the formula 0.52 × length×(width)^2. Statistical analysis was performed with *t*-test (*P ≤ 0.05, **P ≤ 0.01, ***P ≤ 0.001).

effect of virus in MDA-MB-231, most probably due to higher expression of PD-1 on T cell surfaces. Indeed, it is known that all tested cell lines overexpress PD-L1 on their surfaces (40–100%). Also, it has been reported that TNBC (MDA-MB-231 and MDA-MB-468) and non-TNBC cells (MCF-7) upregulate the expression of PD-1 T cells [50]. Oncolytic viruses can be effective in cancer treatment by the lysing of tumour cells and inducing immune system responses. Evidence suggests that oncolytic viruses combined with cancer immunotherapy-based methods, such as immune checkpoint inhibitors, adoptive cell therapies and chemotherapies, can effectively enhance anti-cancer effect. In addition, the efficacy of mono-, dual-, and triple-therapies using oncolytic viruses has been widely published and disseminated [51].

In fact, in our previous preclinical study, we evaluated the antineoplastic activity of combination treatment with SoC chemotherapy (pemetrexed, cisplatin) and oncolytic adenovirus ONCOS-102 in BALB/c xenograft model of human malignant mesothelioma. A synergistic antitumour effect was observed when ONCOS-102 was combined with chemotherapy regimens [10]. This treatment was further tested in the randomized study (EudraCT number 2015-0051430-13), in which patients with unresectable malignant pleural mesothelioma (MPM) received intra-tumorally ONCOS-102 and pemetrexed plus cisplatin/carboplatin, or pemetrexed plus cisplatin/carboplatin alone. The researchers reported a numerical improvement in OS (30-month OS rate 34.1% vs 0; median OS 20.3 vs 13.5 months) with ONCOS-102 compared to chemotherapy alone in chemotherapy-naïve patients (n = 17). By day 36, treatment with the virus was associated with an increase in T-cell infiltration and immune-related gene expression that was not observed in the control group [52]. Our findings are also consistent with previously published results by Sirula et al., where oncolytic adenovirus combined with doxorubicin resulted in improved anti-tumour effect against soft tissue sarcoma (STS) in Syrian hamsters [53].

Taken together, these data highlight that the triple-negative breast cancer line MDA-MB-231 was the most responsive to the anti-cancer treatments, and was therefore selected for the 3D co-culture study.

3.6. 3D co-culture with MDA-MB-231 and PBMCs leads to reduction in TNBC spheroids volume and increase in TILs density

To test the proposed anti-cancer treatments in a more complex cell culture system involving both tumour cells and immune components [54], we generated triple-negative breast cancer spheroids from MDA-MB-231 cells, which we co-cultured with peripheral blood mononuclear cells (PBMCs) from healthy donors (Fig. 5A). PBMCs were selected with HLA matching to the chosen triple-negative breast cancer cell line (A*02:01). HLA compatibility is crucial in order to obtain an integrated system that should simulate the heterogeneity of the tumour microenvironment in order to reproduce the typical interactions between tumour cells and the immune system [55]. The first step, necessary to establish the 3D co-culture model was to verify the effective integration of the immune cells (PBMCs) within the spheroid composed of MDA-MB-231 cells by fluorescence microscopy [54]. In fact, we used bright field and fluorescence imaging to characterize the 3D co-culture (Fig. 5B). Furthermore, we monitored the growth of tumour spheroids before and after PBMCs infiltration by measuring the spheroid areas (Fig. 5B) (average spheroid area on day 3: 58943.21 μm^2 versus average spheroid area after PMBCs addition: 85437.32 μm^2), thus confirming the correct integration of the immune components in the 3D culture system.

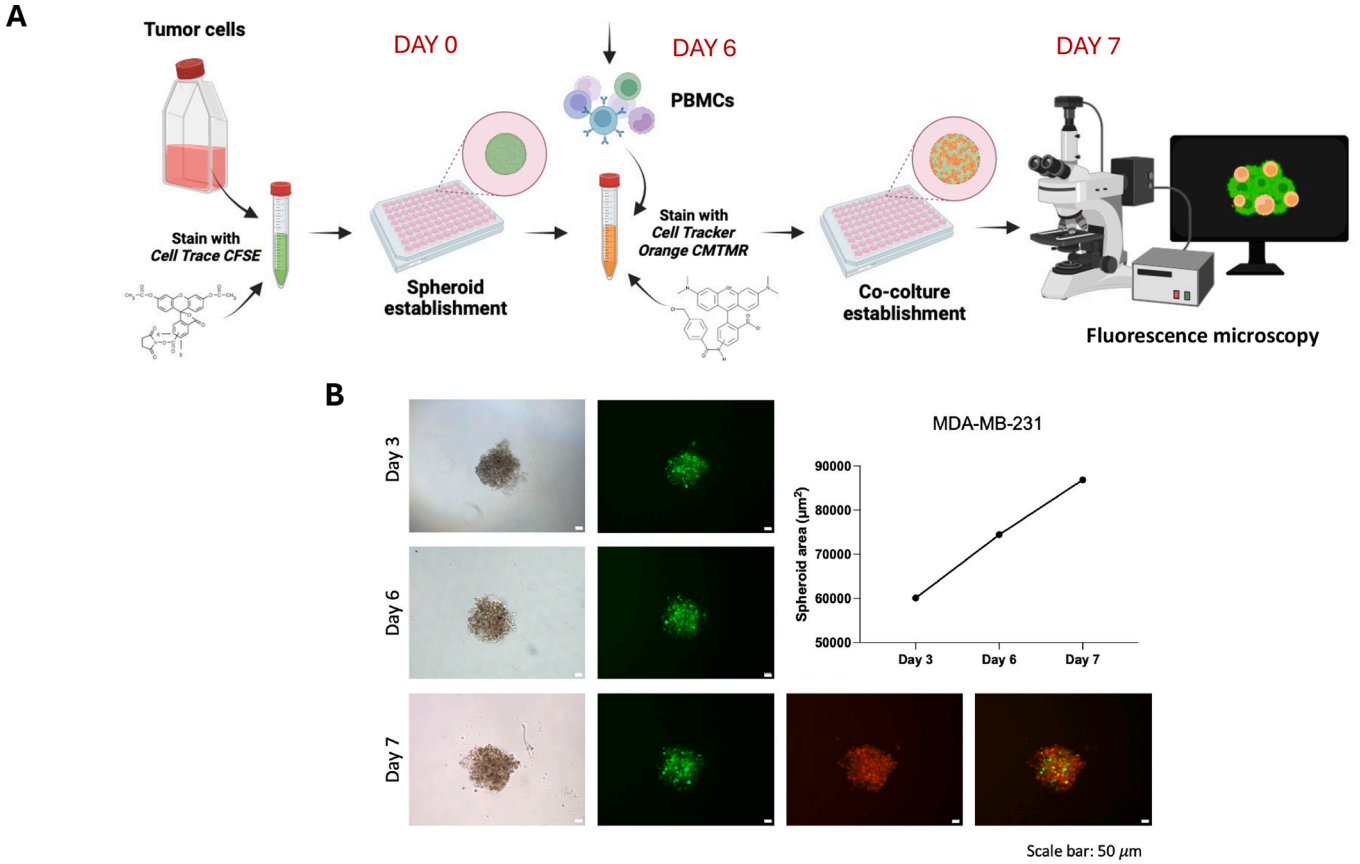

Fig. 5. 3D Co-culture establishment and characterization through fluorescent microscopy. (A-B) MDA-MB-231 cells were stained with Cell Trace CFSE Green and seeded at a density of 1000 cells/well in 96-well plates and centrifuged at 1000 rpm for 5 min to form spheroids. On day 6, PBMCs already stained with CellTracker Orange were added to the tumour spheroids in a 1:1 ratio. After 24 h, images were captured using a fluorescence microscope with 488 and 568 lasers and using 10x objective. Images were assembled using ImageJ software.

Once the 3D co-culture system composed of MDA-MB-231 tumour cells and the immune components deriving from PBMCs was established, we aimed to test the three anti-tumour agents, AdV5/3-D24-ICOSL-CD40L, PTX, pembrolizumab and their combinations according to the treatment schedule presented in Table 3 and Fig. 6A. The results showed that untreated control spheroids continued to grow consistently throughout the entire experiment (spheroid area on day 33: 245892.50 μm^2 and tumour volume: 0.09248 mm^3) (Fig. 6B-C). Nevertheless, compared to previous experiments, where spheroids were composed of MDA-MB-231 tumour cells only, it appears that in this experimental setting, the addition of immune components provided by PBMCs may somehow limit the rapid growth of the spheroids [54].

Interestingly, pembrolizumab administered as monotherapy showed a notable anti-cancer effect, resulting in a spheroid area of 68018.18 μm^2 and a tumour volume of 0.01372 mm^3 at day 33 (Fig. 6B-C, Supplementary Fig. 7). The concentration of pembrolizumab was selected taking into account its clinical dose [56] and dose escalation studies carried out in 3D *in vitro* studies. We can speculate that anti-PD-1 as a monotherapy activated effective T cells in the spheroids. In fact, pembrolizumab regulates changes in T lymphocyte subsets, improving the immune status of patients with a pre-existing immunity. Therefore, monitoring changes in lymphocyte subsets during treatment can predict the effect of immunotherapy [57].

In particular, the double or triple-combination treatment groups showed an improved anti-cancer effect when compared to the monotherapies. These results are consistent with previous studies conducted by the research group in other cancer indications [11,39]. In particular, the combination of the virus and pembrolizumab was able to further reduce both the area and volume of the spheroids as early as at day 16 (spheroid areas: AdV5/3-D24-ICOSL-CD40L as monotherapy: 59240.52 μm^2, Pembrolizumab as monotherapy: 61991.03 μm^2, AdV5/3-D24-ICOSL-CD40L + pembrolizumab: 57298.24 μm^2; spheroids tumour volume: AdV5/3-D24-ICOSL-CD40L as monotherapy: 0.01087 mm^3, pembrolizumab as monotherapy: 0.0119 mm^3, AdV5/3-D24-ICOSL-CD40L + pembrolizumab: 0.0103 mm^3). Moreover, priming with the vector, either followed by the addition of PTX (Priming Virus + PTX spheroid area: 68018.3 μm^2; tumour volume: 0.0137 mm^3) or followed by the administration of both pembrolizumab and then PTX induced improved anti-cancer effects resulting in lower values for both spheroid area and tumour volume (Priming Virus + Pembrolizumab + PTX spheroid area: 37204.19 μm^2; tumour volume 0.0054 mm^3) (Fig. 6B-C) compared to the co-administration treatment strategy (Virus + PTX spheroid area: 87960.6 μm^2; tumour volume: 0.0195 mm^3; Virus + Pembrolizumab + PTX spheroid area: 67500 μm^2; tumour volume: 0.053 mm^3), demonstrating that the proposed strategy could be effective in TNBC patients.

The obtained results are not surprising. It is well known that combination therapy, that employs two or more therapeutic compounds, is a cornerstone of modern cancer treatment. The combination of anti-cancer agents improves efficacy compared to the mono-therapy regime, by targeting fundamental pathways in a characteristically synergistic or additive manner. This potentially minimises drug resistance, while concurrently providing therapeutic anti-cancer benefits such as reducing tumour growth and metastatic potential, arresting mitotically active cells, reducing cancer stem cell populations, triggering apoptosis, ICD and stimulating anti-cancer immunity [58]. In fact, it has been reported that most of the solid tumours express adenovirus cell entry receptors (DSG2) [59]. Therefore, it is anticipated that based on our

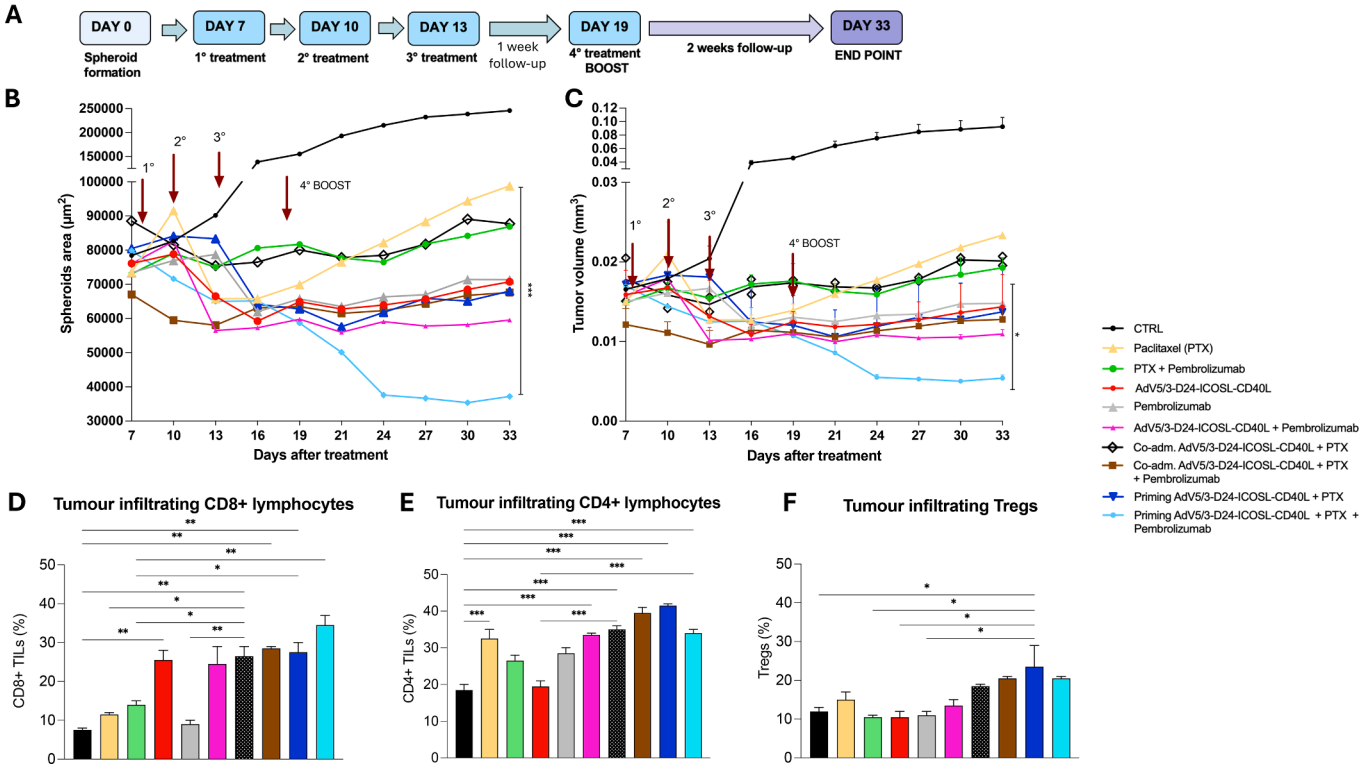

Fig. 6. Assessment of anti-cancer efficacy and immune cell infiltration of tested combinatory therapy on MDA-MB-231 co-culture model. (A) MDA-MB-231 cells were seeded at a density of 1000 cells/well in 96-well plates and centrifuged at 1000 rpm for 5 min to form spheroids. On day 6, PBMCs were added to the tumour spheroids in a 1:1 ratio. The next day, the spheroids were treated with AdV5/3-D24-ICOSL-CD40L (10^9VP/ml), PTX (10 μM), pembrolizumab (150 μg/ml) and their combinations as described in Table 3. Spheroids were examined microscopically every three days. Statistical analysis was performed with *t*-test (*P ≤ 0.05, **P ≤ 0.01, ***P ≤ 0.001). (B-C) Spheroid size was measured on two dimensions every three days, while volume was obtained by applying the formula 0.52 × length × (width)^2. The area was measured using Zeiss AxioVision software. (D-E-F) Levels of tumour infiltrating lymphocytes CD4+, CD8+, Tregs expression in MDA-MB-231 3D co-culture. Samples were collected using BD Lyric FACS Flow. Statistical analyses were carried out with one-way ANOVA test. Error bars, mean ± SEM, *, p ≤ 0.03; **, p ≤ 0.002; ***, p < 0.001.

findings AdV5/3-D24-ICOSL-CD40L can infect, replicate, and lyse cancer cells efficiently. Moreover, based on clinical data, oncolytic virotherapy showed promising clinical efficacy and signs of anti-tumor immunity. Importantly, it has been previously demonstrated that treatment with OVs resulted in the infiltration of CD8+ T cells to tumours and up-regulation of PD-L1, highlighting the potential of oncolytic adenoviruses as an immunosensitizing agent for combinatory therapies with checkpoint inhibitors [60]. Furthermore, it has also been proven that the therapy with oncolytic adenovirus in combination with pembrolizumab resulted in objective responses in patients with anti-PD-1-resistant advanced malignancies [16]. Therefore, due to the OVs unique mode of action we can speculate that combinatory therapy may potentially minimise drug resistance and sensitise for other therapies, including chemotherapy. Taking into account these considerations, in our study, we assessed the efficacy of three different agents exhibiting different, suupplementary anti-cancer efficacy. Therefore, the observed efficacy is based on interplay and interactions between cancer, immune cells, and tested agents, resulting in enhanced efficacy.

Subsequently, as the presence of TILs has been associated with survival benefit in TNBC patients [47], we analysed the nature of TILs in the tumour microenvironment. Increased infiltration of CD8+, CD4+ T and Tregs cells was reported in the groups treated with the double or triple combination regimen (Table 3). However, the highest increase was reported in the group receiving: priming AdV5/3-D24-ICOSL-CD40L + pembrolizumab + PTX (CD8+: p= <.001, vs mock; CD4+: p= <.001, vs mock; Tregs: p = 0,049, vs mock) (Fig. 6D-E-F). A statistically significant correlation was found between tumour volume and CD4+ TILs (Fig. 7, p = 0,037).

In fact, in solid tumors, ICOSL expression promotes the stimulation of CD8+ cytotoxic T cells, resulting in anti-tumor immune function. In

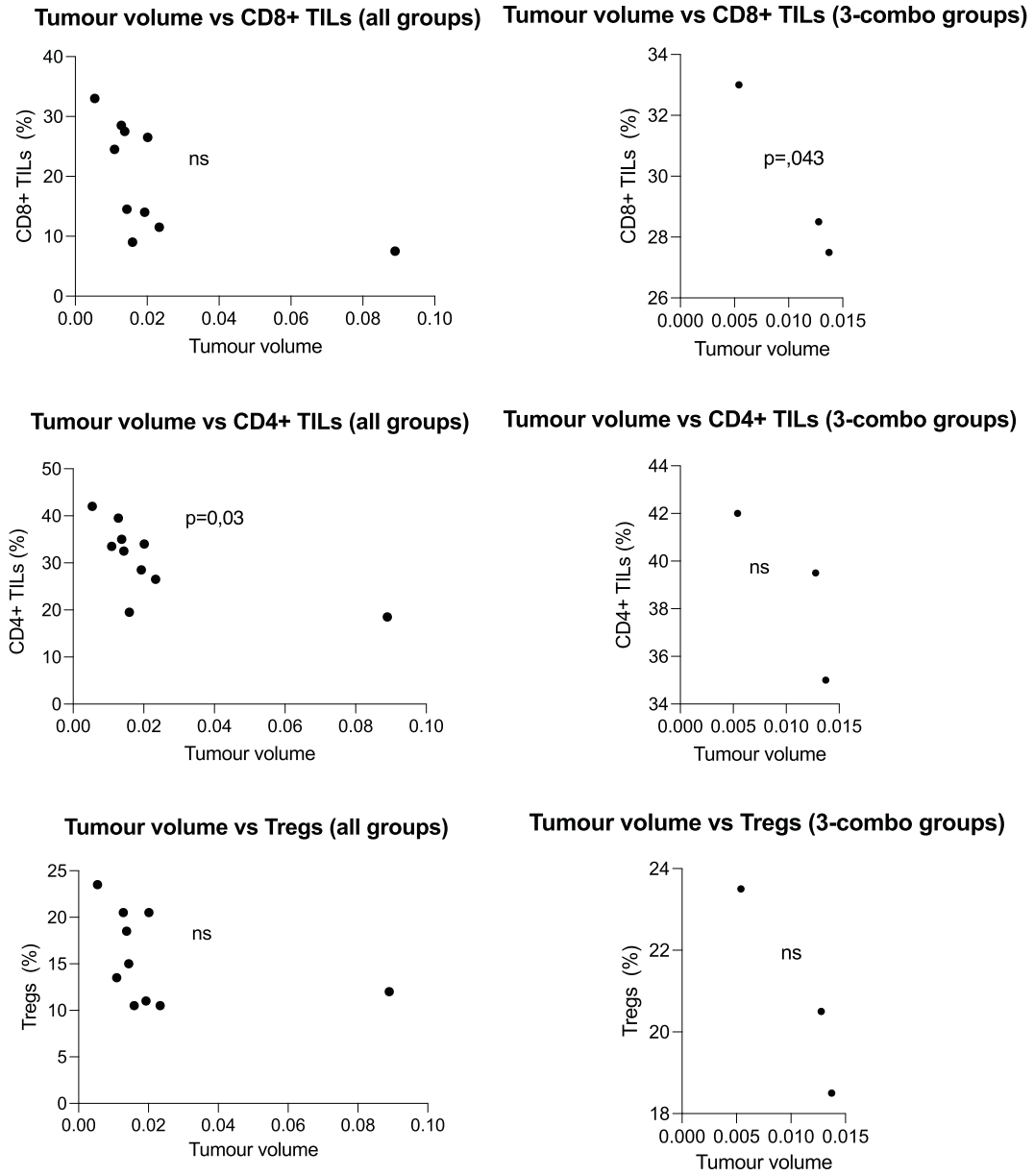

Fig. 7. Immunomodulatory properties of tested agents in MDA-MB-231 3D co-culture. At the end of the study on day 33, tumours were collected for immunological analysis from all tested groups. Tumour infiltrating lymphocytes CD4+, CD8+, Tregs mean expression was assessed in collected tumours. Pearson correlation coefficient was used to identify potential relationships between the mean tumour volume and the mean percentage of CD8+, CD4+, Tregs cells in tumours tissue for all tested groups (left panel) and for triple combinatory groups (right panel). Samples were acquired using BD Lyric FACS Flow. Statistical analyses were performed by ANOVA test, ns – not significant. Error bars, mean ± SEM.

turn, CD40L triggers maturation of antigen presenting cells (APCs). ICOSL transfected tumor cells indicated that the ligand promotes tumor regression by activating CD8+ cytotoxic T-mediated mechanisms [61]. The presence of both co-stimulatory molecules, namely, CD40L and ICOSL, encoded by the virus, most likely contributed to enhanced infiltration of CD4+ and CD8+ T cells in the tumors. In tumour immunity, Treg cells are involved in tumour development and progression by inhibiting anti-tumor immunity. Therefore, an increase in Tregs can be associated with a cancer-self-protection mechanism, trying to fight back and suppress immune responses.

Taken together, these results suggest that the presence of potent co-stimulatory molecules: CD40L and ICOSL, which activate both adaptive [62] and innate immunity [14,63] and are encoded by the vectors, contributed to the increased infiltration of TILs into the tumours. In fact, it has been demonstrated that oncolytic viruses are able to attack immune cells to the tumours. It has previously been described that treatment with AdV5/3-D24-ICOSL-CD40L and anti-PD1 induced enhanced immune cell infiltration that correlated with tumour growth inhibition in mesothelioma mouse models [9]. In addition, Shoushtari et al. reported a pilot study of the oncolytic adenoviral vector, ONCOS-102, administered in combination with pembrolizumab in patients with melanoma resistant to prior PD-1 blockade [16]. Serial biopsies of injected tumours taken at baseline, week 3 (following ONCOS-102 and prior to pembrolizumab), and week 9 (following ONCOS-102 and pembrolizumab) showed that most tumours had increased CD8+ and CD4+ infiltration after the virus injection. Importantly, the TIL infiltration was associated with clinical benefit [16]. Consistent with these findings, the Phase II study in patients with unresectable stage IIIB–IV melanoma with herpes oncolytic virus T-VEC also showed an increase in CD8+ T-cell density in evaluated uninjected lesions. Infiltration also correlated with clinical response, suggesting that T-VEC activates systemic immune activity and modulates the tumour microenvironment [64].

Collectively, our study demonstrated that the combination of different immunotherapeutic agents (virus, pembrolizumab) with PTX was able to reduce the tumour volume of the TNBC co-cultured spheroids compared to relevant controls. Importantly, sequential administration of the investigational agents (priming with the vector) further enhanced the anti-cancer efficacy in 3D culture over other groups tested. Taken together, these results support further evaluation of the virus in combination with anti-PD-1 and PTX for the treatment of triple-negative breast cancer patients.

However, despite these findings, further research aimed at extracting human breast cancer cells directly from patients' biopsies, together with immune cells from their peripheral blood, will be used to generate more complex patient-derived 3D co-culture systems that will allow comprehensive testing of a panel of anti-tumoural agents prior patient administration. Therefore, 3D cultures with patient-derived material could be a model to test new therapeutic strategies that could later be translated into the clinic. As with any model, it is important to be continually aware of its strengths and its limitations. The proposed 3D model has limitations, such as a lack of immunosuppressive TME, a different proportion of the immune system, and a lack of a vascular system. Nevertheless, the system has advantages over standard 2D or a co-culture of PBMCs and 2D cultures, such as the fact that multicellular spheroids provide intermediate complexity between standard culture systems and tumours *in vivo*. Although optimization must be performed, this 3D system can produce important findings in various areas of anti-cancer drug screening. Importantly, comparability studies with *in vivo* models should also be further evaluated and performed to understand translational aspects between different systems.

4. Conclusions

Overall, our study demonstrated that treatment with AdV5/3-D24-ICOSL-CD40L as a priming agent followed by pembrolizumab with paclitaxel was the most effective in reducing the tumour volume of the TNBC co-cultured spheroids. T cell phenotyping analyses revealed significantly enhanced infiltration of CD8+, CD4+ T and Tregs cells, indicating that anti-cancer immunity correlates with the observed efficacy. Our results support the use of three-dimensional (3D) co-culture models to investigate therapeutic efficacy and immune responses of tested compounds. Therefore, 3D models can be considered as a useful tool for anti-cancer drug screening, which should be further exploited and developed.

Funding

The author(s) declare that the financial support was received for the research, authorship, and/or publication of this article. M.G. acknowledges the STARS Starting Grant (STARS StG) (Grant Number: GARO_STARS_MUR22_01) and PRID 2023 (GARO_BIRD23_01) funded by the University of Padua. S.S., P.C., M.G. acknowledge the EU funding within the MUR PNRR "National Center for Gene Therapy and Drugs based on RNA Technology" (Project no. CN00000041, CN3 – Spoke #8 "Platform for DNA/RNA delivery"). L.K. was supported by the National Science Centre, Poland, SONATA (2022/ 47/D/NZ7/03212), The National Centre for Research and Development, Poland, Lider (LIDER14/0258/2023), and the National Institute of Public Health NIH – National Research Institute, Poland (BW-3/2023, 1BWBW/2022).

CRediT authorship contribution statement

Lukasz Kuryk: Writing – review & editing, Writing – original draft, Visualization, Investigation, Formal analysis, Data curation, Conceptualization. **Sara Mathlouthi:** Writing – review & editing, Writing – original draft, Visualization, Investigation, Formal analysis. **Magdalena Wieczorek:** Writing – review & editing. **Beata Gad:** Writing – review & editing. **Beate Rinner:** Writing – review & editing. **Alessio Malfanti:** Writing – review & editing. **Francesca Mastrotto:** Writing – review & editing. **Stefano Salmaso:** Writing – review & editing. **Paolo Caliceti:** Writing – review & editing. **Mariangela Garofalo:** Writing – review & editing, Writing – original draft, Visualization, Validation, Supervision, Resources, Project administration, Methodology, Investigation, Funding acquisition, Formal analysis, Data curation, Conceptualization.

Declaration of Competing Interest

The authors declare the following financial interests/personal relationships which may be considered as potential competing interests: Author LK is an employee and/or shareholder of Valo Therapeutics. The other authors declare that the research was conducted in the absence of any commercial or financial relationship that could be construed as a potential conflict of interest.

Data availability

Data will be made available on request.

Acknowledgements

We thank Elisa Baggio for her precious technical help.

Appendix A. Supplementary data

Supplementary data to this article can be found online at https://doi.org/10.1016/j.ejpb.2024.114300.

References

[1] F. Bray, J. Ferlay, I. Soerjomataram, R.L. Siegel, L.A. Torre, A. Jemal, Global cancer statistics 2018: GLOBOCAN estimates of incidence and mortality worldwide for 36 cancers in 185 countries, CA Cancer J. Clin. 68 (2018) (2018) 394–424.

[2] M. Arnold, E. Morgan, H. Rumgay, A. Mafra, D. Singh, M. Laversanne, J. Vignat, J. R. Gralow, F. Cardoso, S. Siesling, I. Soerjomataram, Current and future burden of breast cancer: global statistics for 2020 and 2040, Breast 66 (2022) 15–23.

[3] H. Sung, J. Ferlay, R.L. Siegel, M. Laversanne, I. Soerjomataram, A. Jemal, F. Bray, Global Cancer Statistics 2020: GLOBOCAN estimates of incidence and mortality worldwide for 36 cancers in 185 countries, CA Cancer J. Clin. 71 (2021) 209–249.

[4] C.M. Perou, T. Sorlie, M.B. Eisen, M. van de Rijn, S.S. Jeffrey, C.A. Rees, J. R. Pollack, D.T. Ross, H. Johnsen, L.A. Akslen, O. Fluge, A. Pergamenschikov, C. Williams, S.X. Zhu, P.E. Lonning, A.L. Borresen-Dale, P.O. Brown, D. Botstein, Molecular portraits of human breast tumours, Nature 406 (2000) 747–752.

[5] R. Dent, M. Trudeau, K.I. Pritchard, W.M. Hanna, H.K. Kahn, C.A. Sawka, L. A. Lickley, E. Rawlinson, P. Sun, S.A. Narod, Triple-negative breast cancer: clinical features and patterns of recurrence, Clin. Cancer Res. 13 (2007) 4429–4434.

[6] C.R. Kennedy, F. Gao, J.A. Margenthaler, Neoadjuvant versus adjuvant chemotherapy for triple negative breast cancer, J. Surg. Res. 163 (2010) 52–57.

[7] J.H. Park, J.H. Ahn, S.B. Kim, How shall we treat early triple-negative breast cancer (TNBC): from the current standard to upcoming immuno-molecular strategies, ESMO Open 3 (2018) e000357.

[8] J. Crown, J. O'Shaughnessy, G. Gullo, Emerging targeted therapies in triple-negative breast cancer, Ann. Oncol. 23 (Suppl 6) (2012) vi56-65.

[9] M. Garofalo, M. Wieczorek, I. Anders, M. Staniszewska, M. Lazniewski, M. Prygiel, A.A. Zasada, T. Szczepinska, D. Plewczynski, S. Salmaso, P. Caliceti, V. Cerullo, R. Alemany, B. Rinner, K. Pancer, L. Kuryk, Novel combinatorial therapy of oncolytic adenovirus AdV5/3-D24-ICOSL-CD40L with anti PD-1 exhibits enhanced anti-cancer efficacy through promotion of intratumoral T-cell infiltration and modulation of tumour microenvironment in mesothelioma mouse model, Front. Oncol. 13 (2023) 1259314.

[10] L. Kuryk, E. Haavisto, M. Garofalo, C. Capasso, M. Hirvinen, S. Pesonen, T. Ranki, L. Vassilev, V. Cerullo, Synergistic anti-tumor efficacy of immunogenic adenovirus ONCOS-102 (Ad5/3-D24-GM-CSF) and standard of care chemotherapy in preclinical mesothelioma model, Int. J. Cancer 139 (2016) 1883–1893.

[11] M. Garofalo, L. Bertinato, M. Staniszewska, M. Wieczorek, S. Salmaso, S. Schrom, B. Rinner, K.W. Pancer, L. Kuryk, Combination therapy of novel oncolytic adenovirus with Anti-PD1 resulted in enhanced anti-cancer effect in syngeneic immunocompetent melanoma mouse model, Pharmaceutics 13 (2021).

[12] L. Kuryk, A.S.W. Møller, Next generation oncolytic viruses expressing PADI1 and TIMP2 exhibit anti-tumor activity against melanoma in nude and humanized mouse models, Mol. Ther. Oncolytics 28 (2023) 158–170.

[13] L. Kuryk, A.W. Moller, A. Vuolanto, S. Pesonen, M. Garofalo, V. Cerullo, M. Jaderberg, Optimization of early steps in oncolytic adenovirus ONCOS-401 production in T-175 and HYPERFlasks, Int. J. Mol. Sci. 20 (2019).

[14] L. Kuryk, A.W. Moller, M. Jaderberg, Quantification and functional evaluation of CD40L production from the adenovirus vector ONCOS-401, Cancer Gene Ther. 26 (2019) 26–31.

[15] M. Garofalo, F. Bellato, S. Magliocca, A. Malfanti, L. Kuryk, B. Rinner, S. Negro, S. Salmaso, P. Caliceti, F. Mastrotto, Polymer coated oncolytic adenovirus to selectively target hepatocellular carcinoma cells, Pharmaceutics 13 (2021).

[16] A.N. Shoushtari, A.J. Olszanski, M. Nyakas, T.J. Hornyak, J.D. Wolchok, V. Levitsky, L. Kuryk, T.B. Hansen, M. Jäderberg, Pilot study of ONCOS-102 and Pembrolizumab: remodeling of the tumor microenvironment and clinical outcomes in Anti–PD-1–resistant advanced melanoma, Clin. Cancer Res. 29 (2023) 100–109.

[17] L. Kuryk, G. Rodella, M. Staniszewska, K.W. Pancer, M. Wieczorek, S. Salmaso, P. Caliceti, M. Garofalo, Novel insights into mesothelioma therapy: emerging avenues and future prospects, Front. Oncol. 12 (2022) 916839.

[18] D. Lin, Y. Shen, T. Liang, Oncolytic virotherapy: basic principles, recent advances and future directions, Signal Transduct. Target. Ther. 8 (2023) 156.

[19] O. Moaven, W.M. C, A.S. J, P.Z. Anastasiadis, M.J. Borad, Evolving role of oncolytic virotherapy: challenges and prospects in clinical practice, JCO Precis. Oncol., 5 (2021).

[20] L. Kuryk, A.W. Moller, M. Jaderberg, Abscopal effect when combining oncolytic adenovirus and checkpoint inhibitor in a humanized NOG mouse model of melanoma, J. Med. Virol. 91 (2019) 1702–1706.

[21] P. Sharma, J.P. Allison, Immune checkpoint targeting in cancer therapy: toward combination strategies with curative potential, Cell 161 (2015) 205–214.

[22] Y. Ren, J. Song, X. Li, N. Luo, Rationale and clinical research progress on PD-1/PD-L1-based immunotherapy for metastatic triple-negative breast cancer, Int. J. Mol. Sci. 23 (2022).

[23] P. Schmid, J. Cortes, R. Dent, L. Pusztai, H. McArthur, S. Kümmel, J. Bergh, C. Denkert, Y.H. Park, R. Hui, N. Harbeck, M. Takahashi, M. Untch, P.A. Fasching, F. Cardoso, Y. Ding, K. Tryfonidis, G. Aktan, V. Karantza, J. O'Shaughnessy, VP7-2021: KEYNOTE-522: phase III study of neoadjuvant pembrolizumab + chemotherapy vs. placebo + chemotherapy, followed by adjuvant pembrolizumab vs. placebo for early-stage TNBC, Ann. Oncol. 32 (2021) 1198–1200.

[24] A.L. Heeke, A.R. Tan, Checkpoint inhibitor therapy for metastatic triple-negative breast cancer, Cancer Metastasis Rev. 40 (2021) 537–547.

[25] K. Mantwill, F.G. Klein, D. Wang, S.V. Hindupur, M. Ehrenfeld, P.S. Holm, R. Nawroth, Concepts in oncolytic adenovirus therapy, Int. J. Mol. Sci. 22 (2021).

[26] Z. Jiang, X. Chen, Y. Lin, Q. Li, X. Nie, G. Xu, C. Yu, X. Zhang, Y. Luan, Synergistic approach to combat triple-negative breast cancer: B7–H4 checkpoint-based photodynamic nanodrug coupled with neutrophil extracellular trap regulation, Adv. Funct. Mater. 33 (2023).

[27] S. Jin, Q. Wang, H. Wu, D. Pang, S. Xu, Oncolytic viruses for triple negative breast cancer and beyond, Biomark Res. 9 (2021) 71.

[28] F. Schettini, M. Giuliano, S. De Placido, G. Arpino, Nab-paclitaxel for the treatment of triple-negative breast cancer: rationale, clinical data and future perspectives, Cancer Treat. Rev. 50 (2016) 129–141.

[29] I. Beyer, R. van Rensburg, A. Lieber, Overcoming physical barriers in cancer therapy, Tissue Barriers 1 (2013) e23647.

[30] E. Blanco, H. Shen, M. Ferrari, Principles of nanoparticle design for overcoming biological barriers to drug delivery, Nat. Biotechnol. 33 (2015) 941–951.

[31] S.L. Jacob, L.A. Huppert, H.S. Rugo, Role of immunotherapy in breast cancer, JCO Oncol Pract 19 (2023) 167–179.

[32] K. Brummel, A.L. Eerkens, M. de Bruyn, H.W. Nijman, Tumour-infiltrating lymphocytes: from prognosis to treatment selection, Br. J. Cancer 128 (2023) 451–458.

[33] C. Lebleu, L. Plet, F. Moussy, G. Gitton, R. Da Costa Moreira, L. Guduff, B. Burlot, R. Godiveau, A. Merry, S. Lecommandoux, G. Errasti, C. Philippe, T. Delacroix, R. Chakrabarti, Improving aqueous solubility of paclitaxel with polysarcosine-b-poly(gamma-benzyl glutamate) nanoparticles, Int. J. Pharm. 631 (2023) 122501.

[34] J. Zhu, Y. Wei, J. Zhang, S. Qian, Y. Gao, W. Heng, Are all poorly soluble drugs dissolved in deep eutectic solvents true solutions? J. Colloid Interface Sci. 645 (2023) 813–822.

[35] E.V. Uspenskaya, T.V. Pleteneva, I.V. Kazimova, A.V. Syroeshkin, Evaluation of poorly soluble drugs' dissolution rate by laser scattering in different water isotopologues, Molecules 26 (2021).

[36] L. Kuryk, A.W. Moller, M. Jaderberg, Combination of immunogenic oncolytic adenovirus ONCOS-102 with anti-PD-1 pembrolizumab exhibits synergistic antitumor effect in humanized A2058 melanoma huNOG mouse model, Oncoimmunology 8 (2019) e1532763.

[37] T.A. Theodossiou, M. Ali, M. Grigalavicius, B. Grallert, P. Dillard, K.O. Schink, C. E. Olsen, S. Walchli, E.M. Inderberg, A. Kubin, Q. Peng, K. Berg, Simultaneous defeat of MCF7 and MDA-MB-231 resistances by a hypericin PDT-tamoxifen hybrid therapy, NPJ Breast Cancer 5 (2019) 13.

[38] Y. Tian, Z. Yao, R.B. Roden, H. Zhang, Identification of glycoproteins associated with different histological subtypes of ovarian tumors using quantitative glycoproteomics, Proteomics 11 (2011) 4677–4687.

[39] M. Garofalo, K.W. Pancer, M. Wieczorek, M. Staniszewska, S. Salmaso, P. Caliceti, L. Kuryk, From immunosuppression to immunomodulation - turning cold tumours into hot, J. Cancer 13 (2022) 2884–2892.

[40] L. Kuryk, A.W. Moller, Chimeric oncolytic Ad5/3 virus replicates and lyses ovarian cancer cells through desmoglein-2 cell entry receptor, J. Med. Virol. 92 (2020) 1309–1315.

[41] S.E. Allison, Y. Chen, N. Petrovic, J. Zhang, K. Bourget, P.I. Mackenzie, M. Murray, Activation of ALDH1A1 in MDA-MB-468 breast cancer cells that over-express CYP2J2 protects against paclitaxel-dependent cell death mediated by reactive oxygen species, Biochem. Pharmacol. 143 (2017) 79–89.

[42] M.C. Bourgeois-Daigneault, L.E. St-Germain, D.G. Roy, A. Pelin, A.S. Aitken, R. Arulanandam, T. Falls, V. Garcia, J.S. Diallo, J.C. Bell, Combination of Paclitaxel and MG1 oncolytic virus as a successful strategy for breast cancer treatment, Breast Cancer Res. 18 (2016) 83.

[43] J. Liu, P. Wang, B. Huang, Q. Cheng, Y. Duan, L. Chen, T. Ma, C. Zhu, D. Li, W. Fan, M. Yu, Effective suppression of triple negative breast cancer by paclitaxel nanoparticles conjugated with transmembrane TNF-alpha monoclonal antibody, Int. J. Pharm. 624 (2022) 121969.

[44] T.M. Abu Samaan, M. Samec, A. Liskova, P. Kubatka, D. Busselberg, Paclitaxel's mechanistic and clinical effects on breast cancer, Biomolecules 9 (2019).

[45] O. Kepp, L. Zitvogel, G. Kroemer, Clinical evidence that immunogenic cell death sensitizes to PD-1/PD-L1 blockade, Oncoimmunology 8 (2019) e1637188.

[46] Z.N. Abbas, A.Z. Al-Saffar, S.M. Jasim, G.M. Sulaiman, Comparative analysis between 2D and 3D colorectal cancer culture models for insights into cellular morphological and transcriptomic variations, Sci. Rep. 13 (2023) 18380.

[47] T. Todo, H. Ito, Y. Ino, H. Ohtsu, Y. Ota, J. Shibahara, M. Tanaka, Intratumoral oncolytic herpes virus G47Δ for residual or recurrent glioblastoma: a phase 2 trial, Nat. Med. 28 (2022) 1630–1639.

[48] F.W. Symmans, Breast cancer response to paclitaxel in vivo, Drug Resist. Updat. 4 (2001) 297–302.

[49] M. Nedeljkovic, A. Damjanovic, Mechanisms of chemotherapy resistance in triple-negative breast cancer-how we can rise to the challenge, Cells 8 (2019).

[50] R. Saleh, S.M. Toor, S. Khalaf, E. Elkord, Breast cancer cells and PD-1/PD-L1 blockade upregulate the expression of PD-1, CTLA-4, TIM-3 and LAG-3 immune checkpoints in CD4(+) T Cells, Vaccines (basel) 7 (2019).

[51] H. Zou, X.Z. Mou, B. Zhu, Combining of oncolytic virotherapy and other immunotherapeutic approaches in cancer: a powerful functionalization tactic, Glob. Chall. 7 (2023) 2200094.

[52] S. Ponce, S. Cedres, C. Ricordel, N. Isambert, S. Viteri, M. Herrera-Juarez, A. Martinez-Marti, A. Navarro, M. Lederlin, X. Serres, J. Zugazagoitia, S. Vetrhus, M. Jaderberg, T.B. Hansen, V. Levitsky, L. Paz-Ares, ONCOS-102 plus pemetrexed and platinum chemotherapy in malignant pleural mesothelioma: a randomized phase 2 study investigating clinical outcomes and the tumor microenvironment, J. Immunother. Cancer 11 (2023).

[53] M. Siurala, S. Bramante, L. Vassilev, M. Hirvinen, S. Parviainen, S. Tahtinen, K. Guse, V. Cerullo, A. Kanerva, A. Kipar, M. Vaha-Koskela, A. Hemminki, Oncolytic adenovirus and doxorubicin-based chemotherapy results in synergistic antitumor activity against soft-tissue sarcoma, Int. J. Cancer 136 (2015) 945–954.

[54] D.P. Saraiva, A.T. Matias, S. Braga, A. Jacinto, M.G. Cabral, Establishment of a 3D co-culture with MDA-MB-231 breast cancer cell line and patient-derived immune

cells for application in the development of immunotherapies, Front. Oncol. 10 (2020) 1543.
[55] C. Jubelin, J. Munoz-Garcia, L. Griscom, D. Cochonneau, E. Ollivier, M. F. Heymann, F.M. Vallette, L. Oliver, D. Heymann, Three-dimensional in vitro culture models in oncology research, Cell Biosci. 12 (2022) 155.
[56] P. Schmid, J. Cortes, L. Pusztai, H. McArthur, S. Kummel, J. Bergh, C. Denkert, Y. H. Park, R. Hui, N. Harbeck, M. Takahashi, T. Foukakis, P.A. Fasching, F. Cardoso, M. Untch, L. Jia, V. Karantza, J. Zhao, G. Aktan, R. Dent, J. O'Shaughnessy, K. Investigators, Pembrolizumab for early triple-negative breast cancer, N. Engl. J. Med. 382 (2020) 810–821.
[57] L. Feng, T.K. Li, K. Yin, S.X. Zhang, Z. Chen, Y. Bao, Effect of pembrolizumab on T lymphocyte subsets in patients with advanced oral cancer and its therapeutic effect, Medicine (Baltimore) 101 (2022) e30534.
[58] R. Bayat Mokhtari, T.S. Homayouni, N. Baluch, E. Morgatskaya, S. Kumar, B. Das, H. Yeger, Combination therapy in combating cancer, Oncotarget 8 (2017) 38022–38043.
[59] L.C.M. Hensen, R.C. Hoeben, S.T.F. Bots, Adenovirus receptor expression in cancer and its multifaceted role in oncolytic adenovirus therapy, Int. J. Mol. Sci. 21 (2020).
[60] T. Ranki, S. Pesonen, A. Hemminki, K. Partanen, K. Kairemo, T. Alanko, J. Lundin, N. Linder, R. Turkki, A. Ristimaki, E. Jager, J. Karbach, C. Wahle, M. Kankainen, C. Backman, M. von Euler, E. Haavisto, T. Hakonen, R. Heiskanen, M. Jaderberg, J. Juhila, P. Priha, L. Suoranta, L. Vassilev, A. Vuolanto, T. Joensuu, Phase I study with ONCOS-102 for the treatment of solid tumors - an evaluation of clinical response and exploratory analyses of immune markers, J. Immunother. Cancer 4 (2016) 17.
[61] B. Wang, H. Jiang, T. Zhou, N. Ma, W. Liu, Y. Wang, L. Zuo, Expression of ICOSL is associated with decreased survival in invasive breast cancer, PeerJ 7 (2019) e6903.
[62] C. Solinas, C. Gu-Trantien, K. Willard-Gallo, The rationale behind targeting the ICOS-ICOS ligand costimulatory pathway in cancer immunotherapy, ESMO Open 5 (2020).
[63] G.L. Beatty, Y. Li, K.B. Long, Cancer immunotherapy: activating innate and adaptive immunity through CD40 agonists, Expert Rev. Anticancer Ther. 17 (2017) 175–186.
[64] J. Malvehy, I. Samoylenko, D. Schadendorf, R. Gutzmer, J.J. Grob, J.J. Sacco, K. S. Gorski, A. Anderson, C.A. Pickett, K. Liu, H. Gogas, Talimogene laherparepvec upregulates immune-cell populations in non-injected lesions: findings from a phase II, multicenter, open-label study in patients with stage IIIB-IVM1c melanoma, J. Immunother. Cancer 9 (2021).